

Abbreviations

%N	percentage nitrogen by mass
a.u.	atomic units
B3LYP	Becke, 3-parameter, Lee-Yang-Parr hybrid functional
BCP	bonding critical point
CH₃CH₃	NC repeat unit with two methoxy capping groups
CH₃OH	NC repeat unit with methoxy capping group on ring 1, hydroxy group on ring 2
CCP	cage critical point
CP	critical point
DFT	density functional theory
DOS	degree of substitution
EM	energetic materials
ESP	electrostatic potential
G09	Gaussian 09 revision D.01
GM	genetically modified
GView	Gauss View 5.0.8
HF	Hartree Fock theory
IR	infra-red spectroscopy

MEP	minimum energy path
MM	molecular mechanics
MMFF94	Merck molecular force field 94
MW	molecular weight
NC	nitrocellulose
NCP	nuclear critical point
NG	nitroglycerine
NMR	nuclear magnetic resonance spectroscopy
OHCH₃	NC repeat unit with hydroxy capping group on ring 1, methoxy group on ring 2
PCM	polarisable continuum model
PES	potential energy surface
PETN	pentaerythritol tetranitrate
QM	quantum mechanics
QTAIM	quantum theory of atoms in molecules
RCP	ring critical point
SB59	1,4-bis(ethylamino)-9,10-anthraquinone dye
SEM	scanning electron microscopy
S_N2	bi-molecular nucleophilic substitution reaction
TS	transition state
UFF	universal force field
UV	ultraviolet
UV-Vis	ultraviolet-visible spectroscopy
ωB97X-D	ω B97X-D long-range corrected hybrid functional

Chapter 2

Nitration and Denitration Sequence of Nitrocellulose

[Added as preamble for Chapter 4 below]

2.1 Introduction

Moniruzzaman *et al.* used the UV absorption of an anthraquinone dye to determine the activation energies for the removal of the nitrate at C2, C3, C6 sites on nitrocellulose (NC) (figure 2.1)[1]. UV-Vis was chosen as an efficient, non-destructive method of monitoring the decomposition process. The reaction of the 1,4-bis(ethylamino)-9,10-anthraquinone dye (SB59) with NO_x released by denitration mimics the action of stabilisers within NC formulations. The dye consume any nitrates released in the system, eliminating the possibility of successive reactions generating acidic species. Decreasing peak intensity of the dye and appearance of new absorption regions gave insight into the extent of denitration and the presence of secondary reaction products. The presence of acid has been linked to autocatalytic rates of degradation during later stages of NC degradation[2, 3, 4, 5].

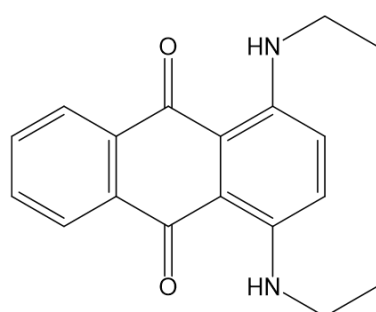


Figure 2.1: 1,4-bis(ethylamino)-9,10-anthraquinone dye (SB59) used to probe the release of nitrates from NC using UV-Vis and ¹H NMR spectroscopy[1]. Following reaction with NO_x, the UV absorption peak of the dye is depleted.

Un-aged NC thin films and films aged at 40°C, 50°C, 60°C and 70°C for timescales of up to 2000hrs for 40°C, were compared. The NC starting material was 12.15%N by mass, with mean degree of substitution (DOS)=2.307, indicating that individual glucopyranose rings were of mixed nitration level with non-uniform distribution of nitrate groups along the polymer. The study found that the nitrate at the C3 position would be most reactive, possessing the lowest activation barrier to removal. This was followed by C2 and C6. The findings contrast with the computational work of Shukla *et al.*, who determined that denitration via alkylaline hydrolysis followed the order of C3→C6→C2 [6, 7]. In this case, the study only considered the fully nitrated system. There is evidence that nitration and denitration are influenced by the presence of nitrate groups at adjacent positions. Matveev *et al.* demonstrated that for polynitro esters the rate of liquid-phase decomposition did not increase linearly with number of nitrate reaction centres, but was mainly dependent on individual structures table 4.1[8]. It was suggested that the trend in reactivity could be explained by the inductive effect of nitrate groups.

Table 2.1: Comparison of the rate constants of decomposition, for various polynitrate esters at 140°C. Collated from various literature sources by Matveev *et al.*[8].

Compound	ΔT / °C	E / kcal mol ⁻¹	logA [s ⁻¹]	k _{expt} / 10 ⁻⁶ s ⁻¹
a) O ₂ NOCH ₂ CH ₂ ONO ₂ (nitroglycol)	-	-	-	4.7
b) O ₂ NOCH ₂ CH ₂ CH ₂ ONO ₂	72–140	39.1	14.9	1.7
c) O ₂ NOCH ₂ CH(ONO ₂)(CH ₃)	72–140	40.3	15.8	3.0
d) O ₂ NOCH ₂ CH(OH)(CH ₂ ONO ₂)	80–140	42.4	16.8	2.3
e) O ₂ NOCH ₂ CH ₂ CH ₂ CH ₂ ONO ₂	100–140	39.0	14.7	1.1
f) O ₂ NOCH(CH ₃)CH(CH ₃)ONO ₂	72–140	40.3	14.9	5.0
g) O ₂ NOCH ₂ CH ₂ OCH ₂ CH ₂ ONO ₂	80–140	42.0	16.5	1.9
h) O ₂ NOCH ₂ CH ₂ (NNO ₂)CH ₂ CH ₂ ONO ₂	80–140	41.5	16.5	3.5
i) [(O ₂ NOCH ₂)CH(ONO ₂)CH(ONO ₂)] ₂ (hexanitromannite)	80–140	38.0	15.9	63.0
j) (O ₂ NOCH ₂) ₄ C(TEN)	145–171	39.0	15.6	9.3
k) (O ₂ NOCH ₂) ₂ CHONO ₂	-	-	-	13.0

The inductive effect arises when a difference in the electronegativity between atoms connected by a σ -bond leads to a polarisation, or permanent dipole, in the bond. Electron donating groups increase the $\delta-$ partial charge on neighbouring atoms through the release of electrons, whilst electron withdrawing groups pull electron density away from neighbouring atoms generating a $\delta+$ charge on connected atoms. From the studies above, it is seen that

the denitration order of NC can be influenced by the location, distribution and saturation of the nitrated sites along the polymer, as well as mechanistic differences in thermal and chemical degradation. Crucially, a synergistic effect leading to facile removal of the C3 group when the C2 site is also nitrated may play an important part in the decomposition pathway. The DOS of the source NC would therefore give an indication of the likelihood of adjacent nitrates.

Chapter 4

Post-Denitration Reactions

4.1 Introduction

Following the primary denitration step, products are evolved as gases or remain in the NC matrix. Reactive nitrogen dioxide radicals generated from homolysis of the O-N bond are likely to migrate within the bulk and attack other sites in the polymer . Nitrous acid released from intramolecular reactions within the polymer contribute to the acidity of the overall system, lowering the pH and further stimulating hydrolysis processes.

Neutral and alkaline hydrolysis reactions follow a pseudo-first order process. As described in section 2.1, Moniruzzaman *et al.* used the reaction of nitrates with anthraquinone dye SB59 to probe the reactivity at each of the C2, C3 and C6 sites on NC, using **UVVIS!** (**UVVIS!**) and ^1H NMR spectroscopy (figure 4.1). High concentrations of secondary reaction products following the liberation of the nitrate group were observed. Samples with longer ageing time presented spectra dominated by consecutive products. Though figure 4.1 illustrates the reaction of the dye with NO groups, the study makes no indication of the source of NO_x , except that they are products of thermolysis of NC.

In this section, secondary and extended reaction schemes for the low temperature ageing of NC are explored. Mechanisms proposed by Camera *et al.* and Aellig *et al.* are probed to determine the reactions responsible for the experimentally observed degradation products.

4.2 Methodology

The species reactions proposed by Camera and Aellig *et al.* were geometry optimised using $\omega\text{B97X-D}$ long-range corrected hybrid functional ($\omega\text{B97X-D}$), and Becke, 3-parameter, Lee-Yang-Parr hybrid functional (B3LYP) functionals. The reactions were initially modelled

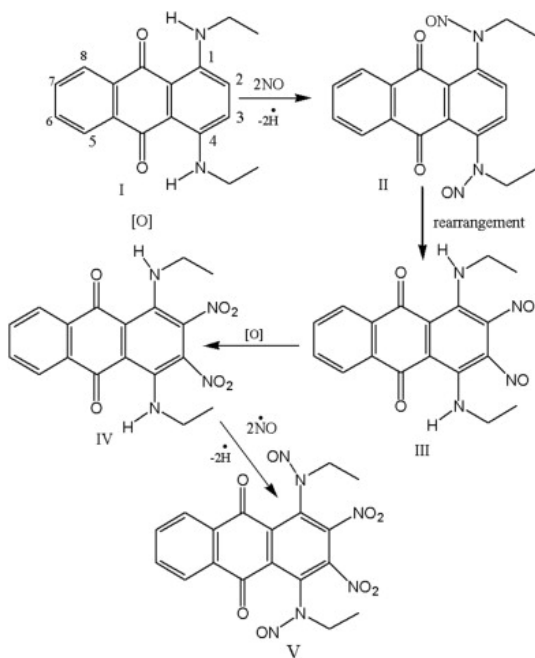


Figure 4.1: Proposed reaction pathway for anthraquinone dye (SB59) with NOx released as a result of denitration, from the work of Moniruzzaman *et al.*[1].

using ethyl nitrate as a test system before expansion to the full C2 monomer.

4.2.1 Computational details

All geometry optimisations were performed in Gaussian 09 revision D.01 (G09), using the ω B97X-D and B3LYP functionals. Optimisations were repeated with polarisable continuum model (PCM) to introduce solvent effects.

4.3 Results and Discussion

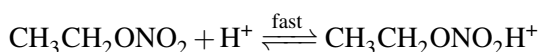
4.3.1 Thermodynamics of Ethyl Nitrate reactions

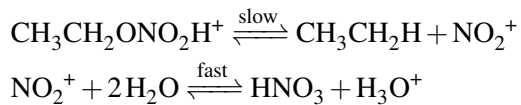
Table 4.1: Free energies of protonation at different oxygens sites on ethyl nitrate.

protonation site	ΔG_r		ΔH_r	
	ω B97X-D	PCM	B3LYP	PCM
Terminal (up) O $\text{CH}_3\text{CH}_2\text{ONO}_2\text{H}^+$	0.0072	0.0083	0.0064	0.0077
Terminal (down) O	-0.0195	0.0140	-0.0219	0.0101
Bridging O	-0.0195	0.0140	-0.0219	0.0101

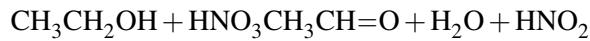
Camera' equations

Hydrolysis

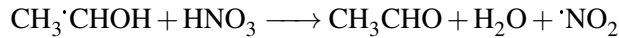
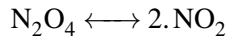
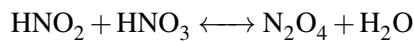




Initiation

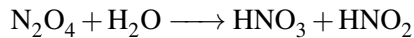
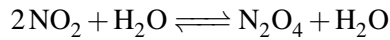


Propagation

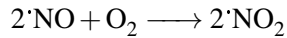
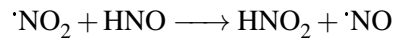
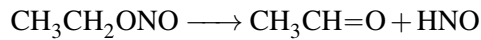
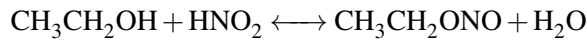


Aellig's equations

Initiation



Propagation



Termination



4.3.1.1 Radical mechanistic route

4.3.1.2 Ionic mechanistic route

4.3.2 Reactions of Nitrocellulose Monomer

4.4 Summary

Bibliography

- [1] Mohammed Moniruzzaman, John M. Bellerby, and Manfred A. Bohn. Activation energies for the decomposition of nitrate ester groups at the anhydroglucopyranose ring positions C2, C3 and C6 of nitrocellulose using the nitration of a dye as probe. *Polymer Degradation and Stability*, 102:49–58, apr 2014.
- [2] M. Edge, N.S. Allen, M. Hayes, P.N.K. Riley, C.V. Horie, and J. Luc-Gardette. Mechanisms of deterioration in cellulose nitrate base archival cinematograph film. *European Polymer Journal*, 26(6):623–630, jan 1990.
- [3] M^a Ángeles Fernández de la Ossa, María López-López, Mercedes Torre, and Carmen García-Ruiz. Analytical techniques in the study of highly-nitrated nitrocellulose. *TrAC Trends in Analytical Chemistry*, 30(11):1740–1755, dec 2011.
- [4] John W. Baker and D. M. Easty. Hydrolytic decomposition of esters of nitric acid. Part I. General experimental techniques. Alkaline hydrolysis and neutral solvolysis of methyl, ethyl, isopropyl, and tert.-butyl nitrates in aqueous alcohol. *Journal of the Chemical Society (Resumed)*, 1952(0):1193–1207, 1952.
- [5] N. Binke, L. Rong, Y. Zhengquan, W. Yuan, Y. Pu, Hu Rongzu, and Y. Qingsen. Studies on the Kinetics of the First Order Autocatalytic Decomposition Reaction of Highly Nitrated Nitrocellulose. *Journal of Thermal Analysis and Calorimetry*, 58(2):403–411, 1999.
- [6] Manoj K. Shukla and Frances Hill. Theoretical investigation of reaction mechanisms of alkaline hydrolysis of 2,3,6-trinitro- β -d-glucopyranose as a monomer of nitrocellulose. *Structural Chemistry*, 23(6):1905–1920, apr 2012.

- [7] Manoj K Shukla and Frances Hill. Computational elucidation of mechanisms of alkaline hydrolysis of nitrocellulose: dimer and trimer models with comparison to the corresponding monomer. *The journal of physical chemistry. A*, 116(29):7746–55, 2012.
- [8] V. G. Matveev and G. M. Nazin. Stepwise Degradation of Polyfunctional Compounds. *Kinetics and Catalysis*, 44(6):735–739, nov 2003.